Figure S1. Oral mucosa organoids can be established from mouse tongue epithelium.

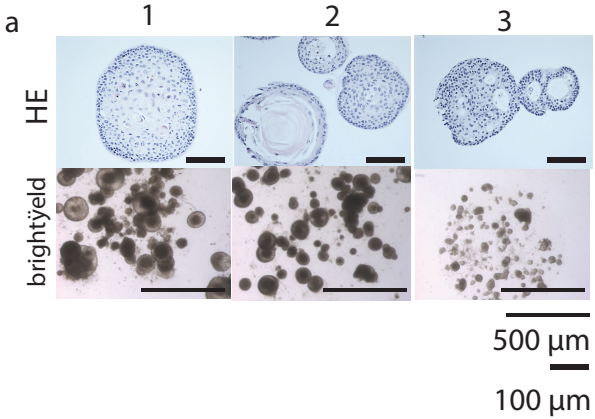

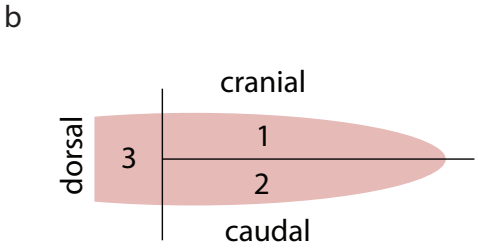

Figure S1. Oral mucosa organoids can be established from mouse tongue epithelium, related to Figure 1. A. brightfield microscopy images and H&E staining of paraffin-embedded organoid sections of organoids established from different regions of the mouse tongue (annotated 1, 2 and 3, see schematic in B) Organoids keratinize at larger sized, revealed by darker centers in the brightfield images or acellular parts in the H&E staining. Scalebar top panels 100 micrometer, scalebar bottom panels 500 micrometer. B. Schematic of locations annotated 1, 2 and 3 in Figure S1A.

Figure S2. Outgrowth of human oral mucosa organoids and characterization using scanning electron microscopy and transmission electron microscopy.

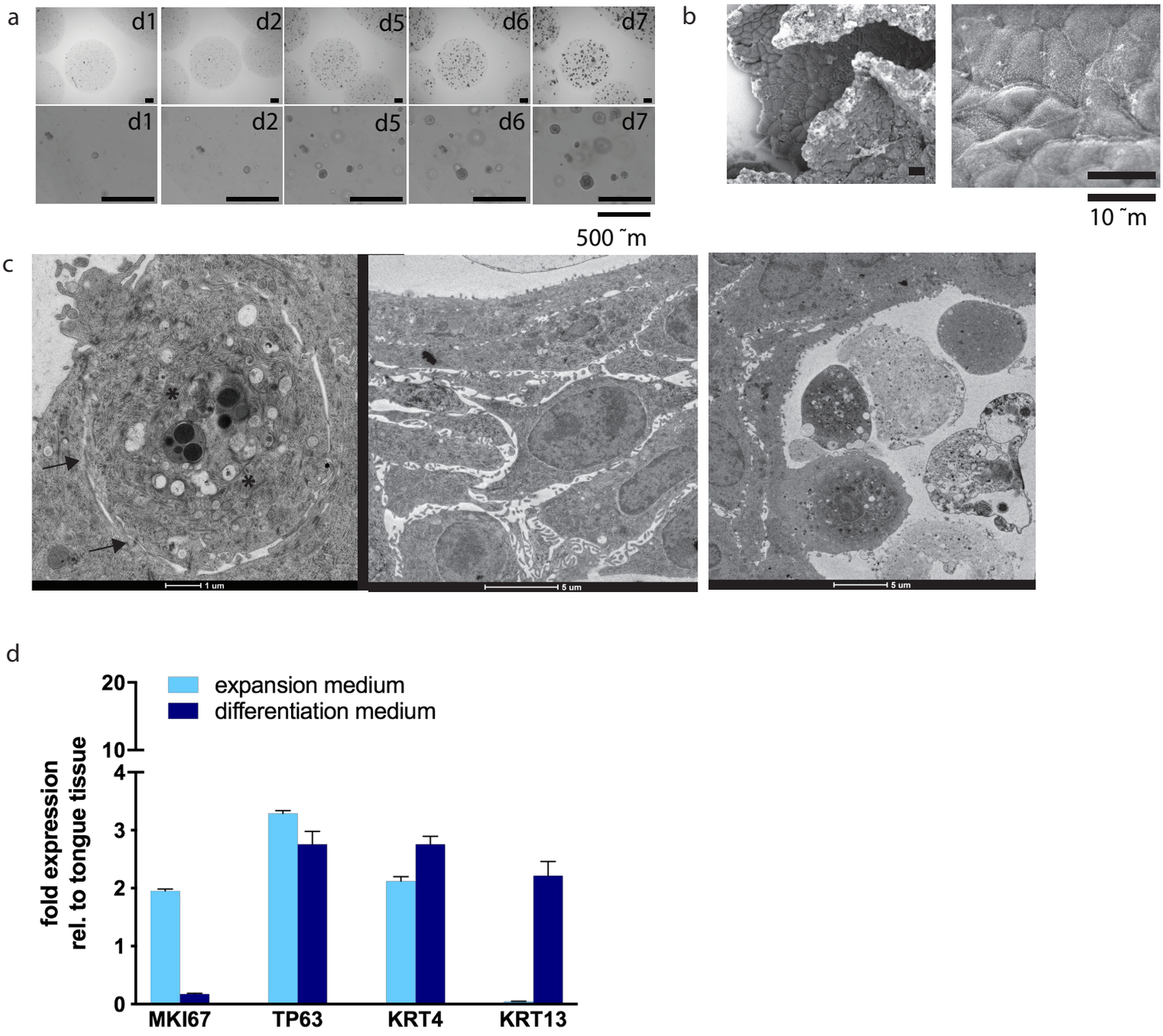

Figure S2. Outgrowth of human oral mucosa organoids and characterization using scanning electron microscopy and transmission electron microscopy, related to Figure 1. A. Organoid outgrowth can be observed from human primary tissue when put in culture. Representative images of establishment of an organoid culture. Starting one day after initial plating of the tissue, images of the same BME drop with human cells were taken on day 1, 2, 5, 6 and 7 to show outgrowth of organoids from primary tissue. Scalebar 500 micrometer. B. Scanning electron microscopy of human oral mucosa organoids. First panel: an organoid that broke open during processing shows the apical surface of organoid cells. Most cells have a smooth surface, whereas some cells have a folded apical surface. Second panel: zoom in of the apical surface of an organoid, showing multiple keratinocytes forming tight connections. Scalebar 10 micrometer C. Transmission electron microscopy images of human oral mucosa organoids. First panel: a single keratinocyte shows properties characteristic for keratinocytes, such as abundant tonofilament formation (asterixes) and tight junctions (arrows) connecting it to neighboring cells. Second panel: cross section spanning the apical part of the organoid wall. Cells located more towards the outside of the organoids are bigger, more rounded and have intact nuclei. Moving more towards the inside of the organoid, cells seem to flatten out, and lose their nucleus. Third panel, cross section showing the inside of an organoid, where cell fragments are still present. One keratinocyte is being shed into the inside of the structure. Scalebars are shown below each individual panel. D. Quantitative PCR of a normal oral mucosa organoid line (N8) for proliferation marker MKI67, basal cell marker TP63 and KRT13, Prior to RNA collection, growth factors were withdrawn from the medium to induce differentiation. Expression levels are calculated using delta Ct method. For each marker, fold change in expression is made relative to expression of this markers in human primary tongue tissue, which is set to 1. n=3, individual data points are shown, bars represent average.

Figure S3. Oral mucosa organoids can be infected with Herpes Simplex Virus and Human Papiloma Virus.

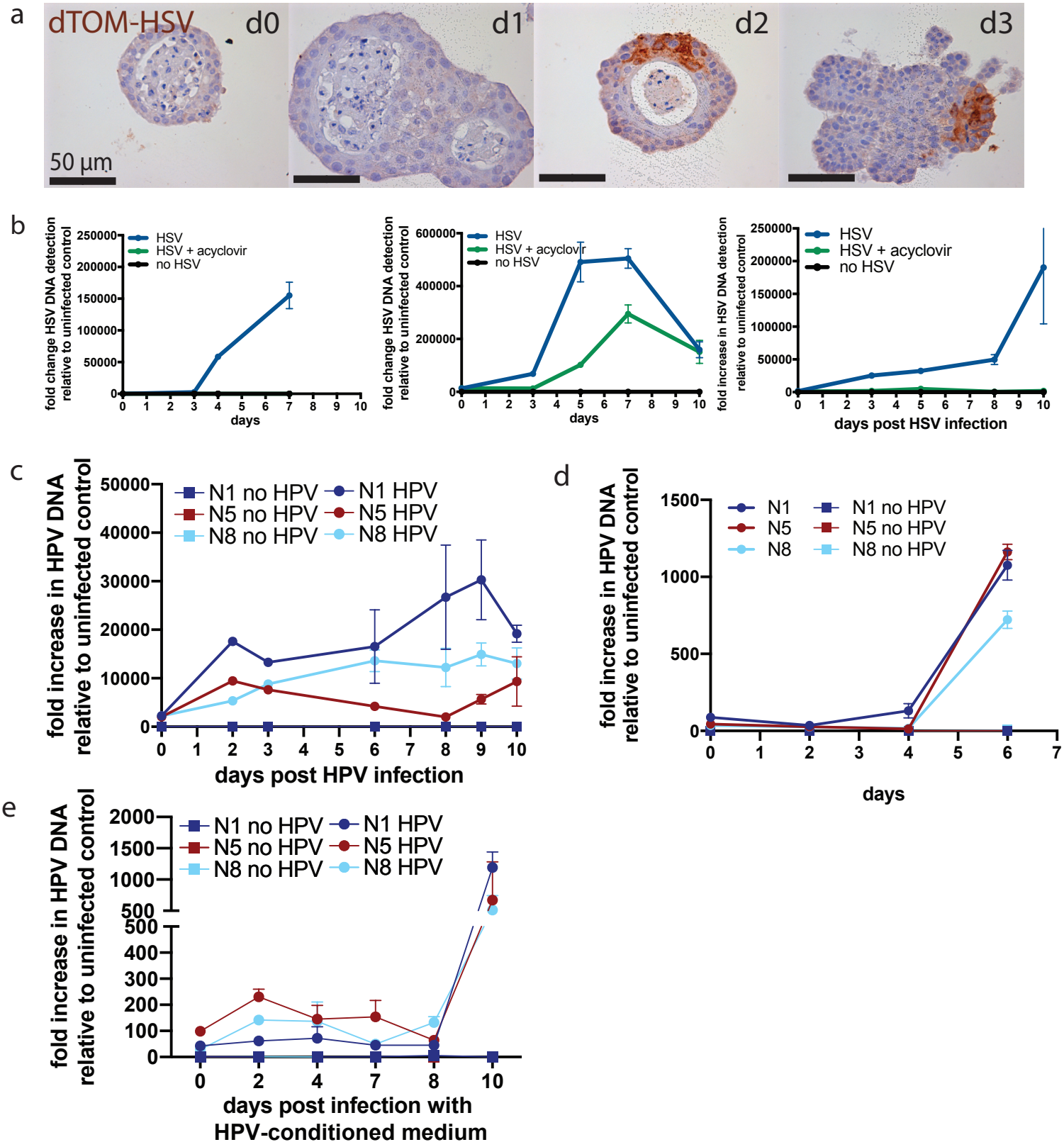

Figure S3. Oral mucosa organoids can be infected with Herpes Simplex Virus and Human Papilloma Virus, related to Figure 1. A. Immunohistochemical staining for dTomato was performed on organoids infected with dTomato labelled HSV (dTOM-HSV). Organoids were collected on day 0, 1, 2 and 3. Scalebar 50 µm. B. Quantification of HSV DNA after infection of oral mucosa organoids derived from three different donors. Quantitative PCR of DNA obtained from oral mucosa organoids infected with HSV and kept in culture for 10 days. HSV can replicate in oral mucosa organoids, and this replication can be inhibited by the addition of acyclovir. Fold increase in DNA content is calculated relative to Ct values of the uninfected control at day 0, using delta Ct method. Datapoints represent the average of three technical replicates, error bars represent the SEM. Blue, organoids infected with HSV. Green, organoids infected with HSV and cultured in the presence of 1 µM acyclovir. Black, organoids not infected with HSV. C. Quantification of HPV DNA after splitting of HPV-infected organoids. 10 days after initial infection (results shown in Figure 2F), organoids were split and plated to follow HPV DNA over time. Increase in HPV DNA could be observed six days after splitting in all three organoid lines. D and E. Quantitative PCR for HPV on DNA obtained from oral mucosa organoids infected with HPV (D) or HPV-conditioned medium (E) and kept in culture for a maximum 10 days. Fold increase in DNA content is shown relative to uninfected control at day 0. Data points represent the average of three technical replicates, error bars represent the SEM.

Figure S4. Brightÿeld images of HNSCC-derived organoid lines.

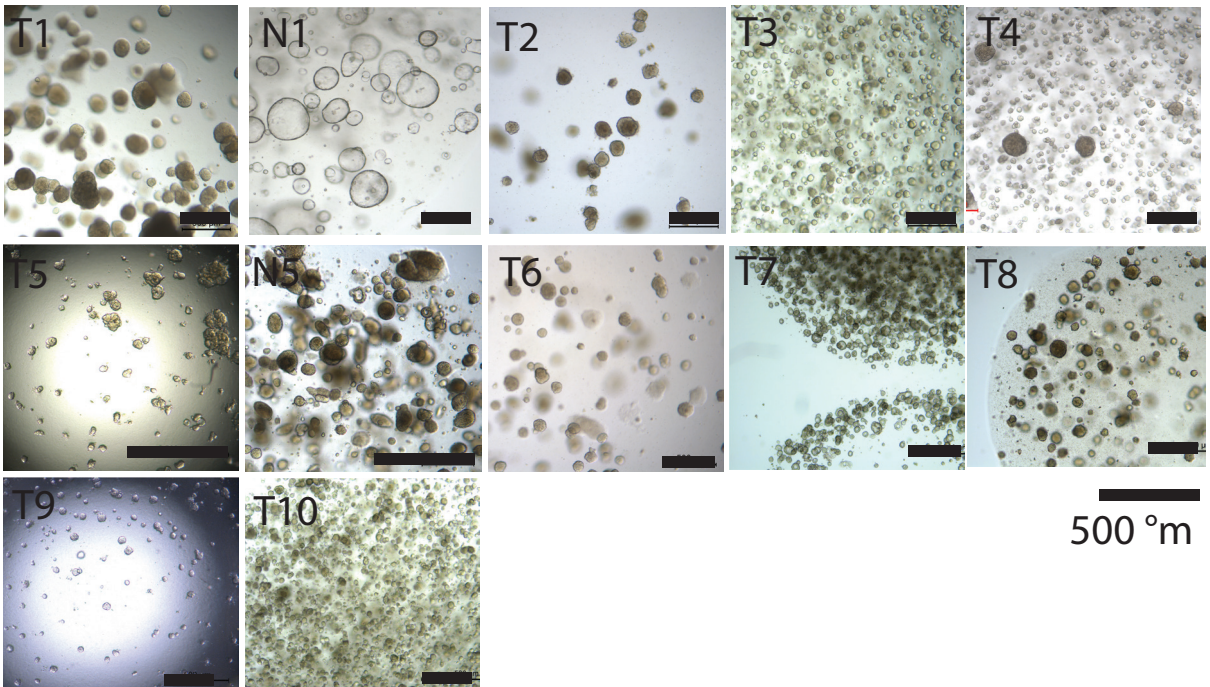

Figure S4. Brightfield images of HNSCC-derived organoid lines, related to Figure 2. For all organoid lines characterized in this work, images are shown of organoids in culture. Scalebar, 500 µm.

Figure S5. H&E staining of HNSCC-derived organoids reveals di˜erences in morphology between di˜erent organoid lines.

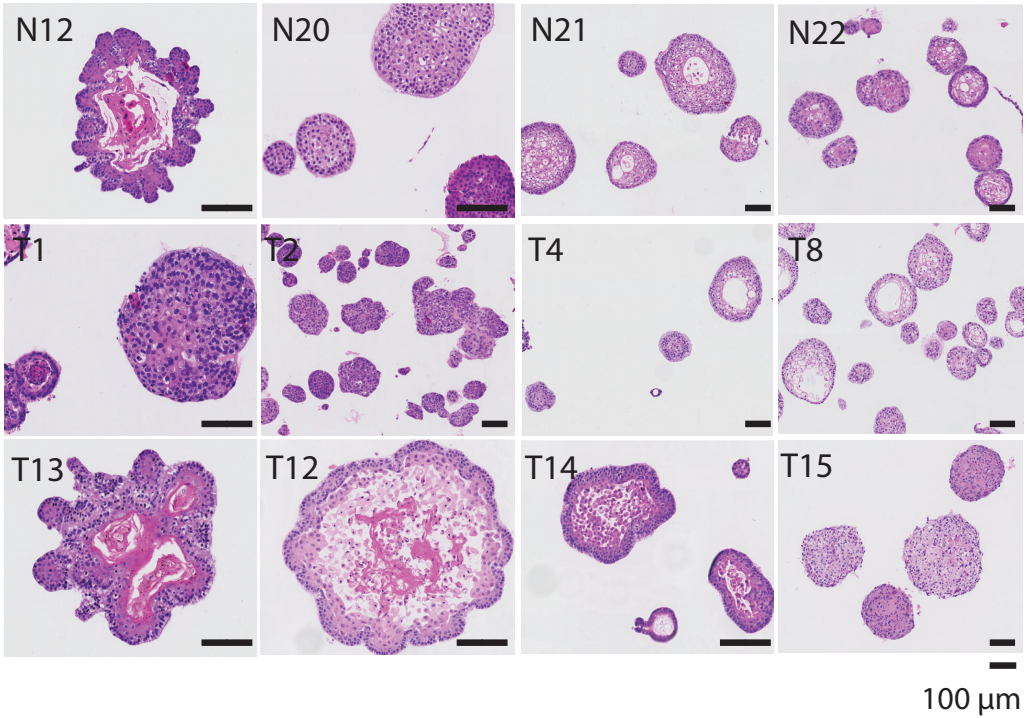

Figure S5. H&E staining of HNSCC-derived organoids reveals differences in morphology between different organoid lines, related to Figure 2. H&E staining performed on sections of paraffin-embedded organoids. Here, H&E staining of four normal and eight tumor lines are shown. Scalebar 100 µm.

Figure S6. Normal and tumor organoids derived from the same patient show di˜ erent morphology.

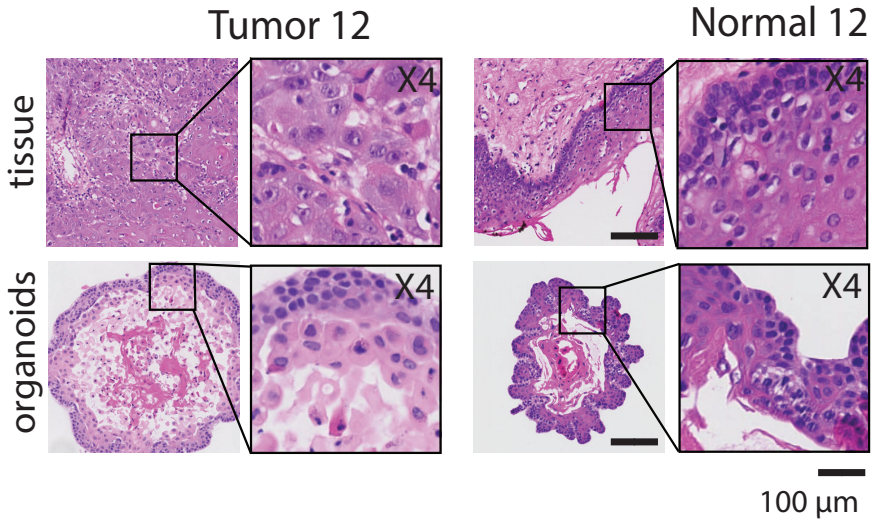

Figure S6. Normal and tumor organoids derived from the same patient show different morphology, related to Figure 2. Organoids were derived from both tumor tissue and adjacent normal tissue from the same patient. H&E staining of organoids are shown and reveal different morphology of the two organoid lines. Scalebar 100 µm.

Figure S7. HNSCC-derived organoid show di˜ erences in sensitivity to Nutlin-3.

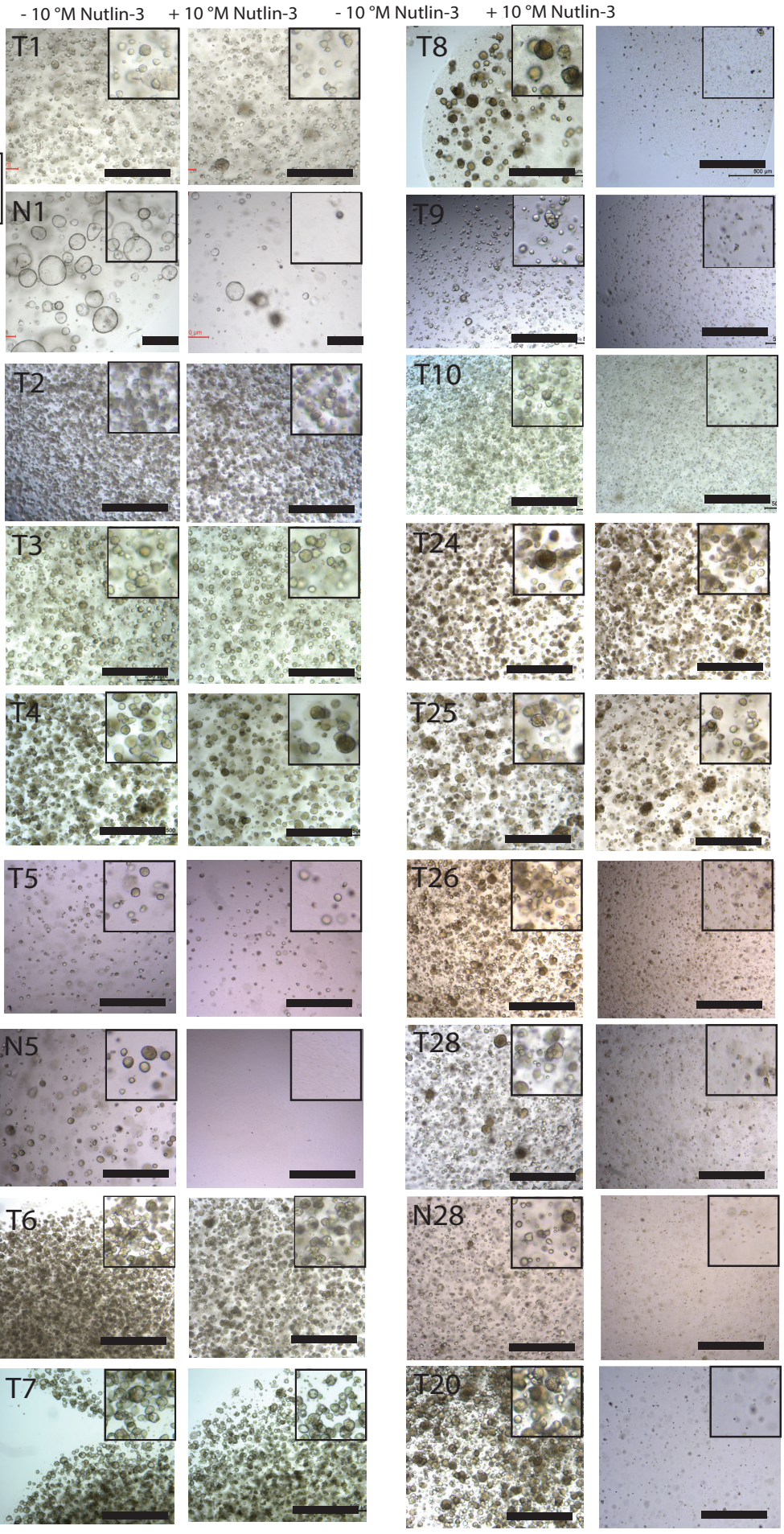

Figure S7. HNSCC-derived organoid show differences in sensitivity to Nutlin-3, related to Figure 2. Organoids were cultured for three passages in the presence of 10 µM Nutlin-3 and passaged weekly. Left panels, organoid cultured in the absence of Nutlin-3. Right panels, organoids cultured in the presence of Nutlin-3. All tumor lines, except T8, T9, T10, T20, T26 and T28 are resistant to these compounds. Both normal lines (N1 and N5, corresponding normal organoids of T1 and T5) show Nutlin-3 sensitivity. Scalebar, 500 µm.

Figure S8. Highlighted genes that are di˜ erentiatlly expressed between normal and tumor organoids.

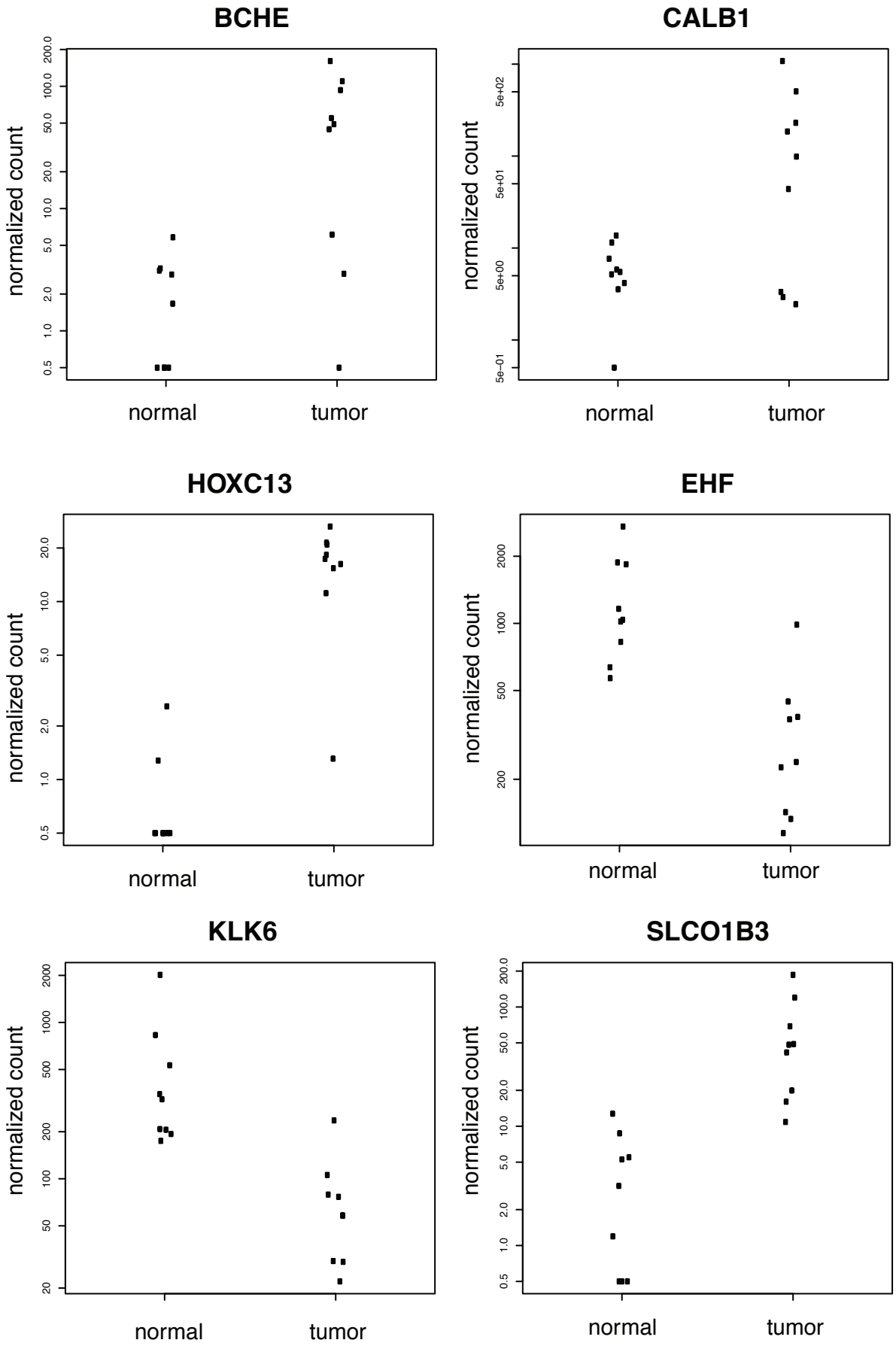

Figure S8. Highligted genes that are differentially expressed between normal and tumor organoids , related to Figure 2. Scatterplots of the expression of these six genes, plotted for each individual gene.

Figure S9. Comparison of sequencing results of primary tissue and organoid cultures of patient 3, 5 and 8.

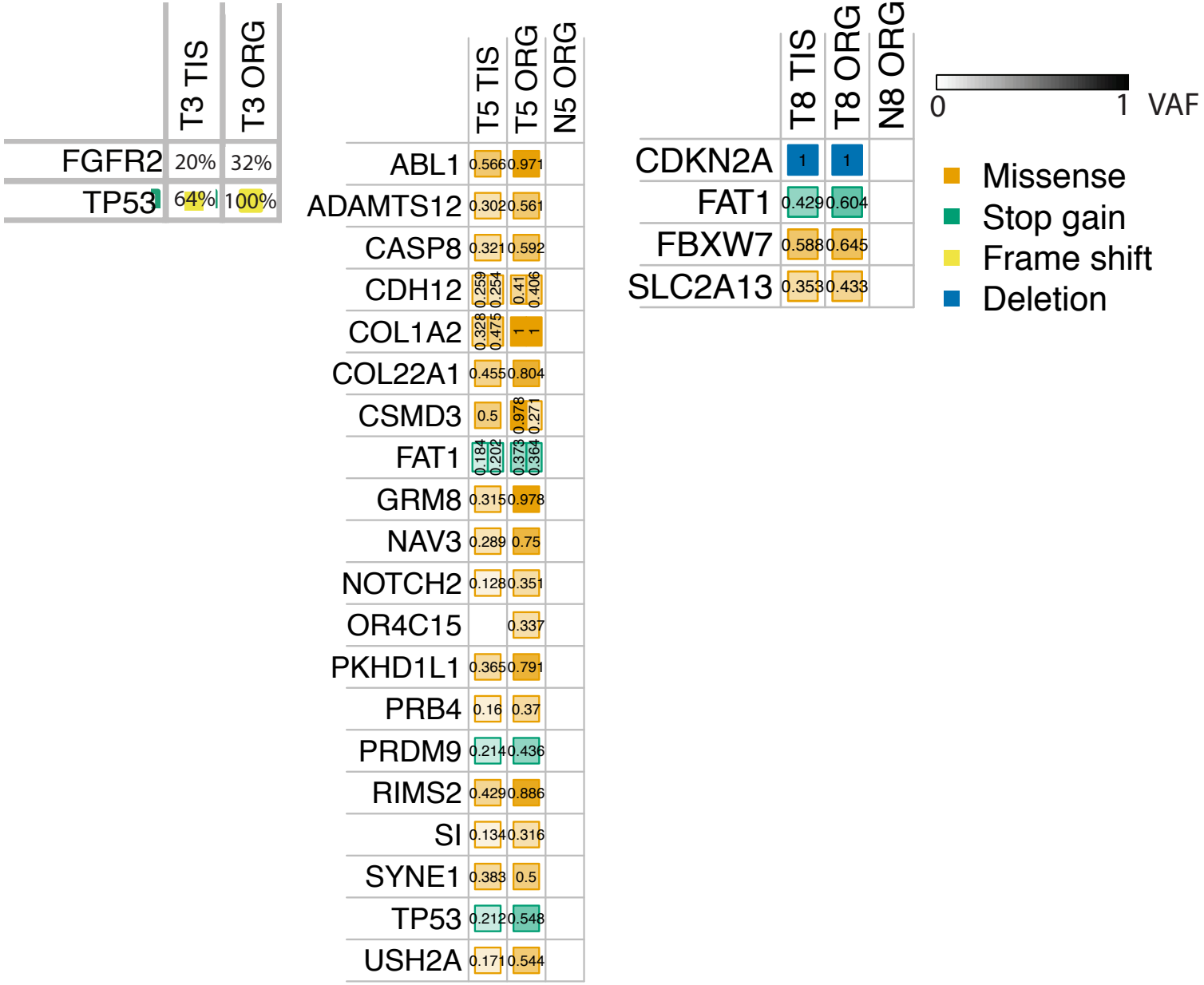

Figure S9. Comparison of sequencing results of primary tissue and organoid cultures of patient 3, 5 and 8, related to Figure 3.
Allele frequency of mutations detected by targeted sequencing (T3) or whole exome sequencing (T5 and T8), performed in both primary tissue and corresponding organoids.

FIgure S10. HNSCC-derived organoids result in tumor formation in vivo.

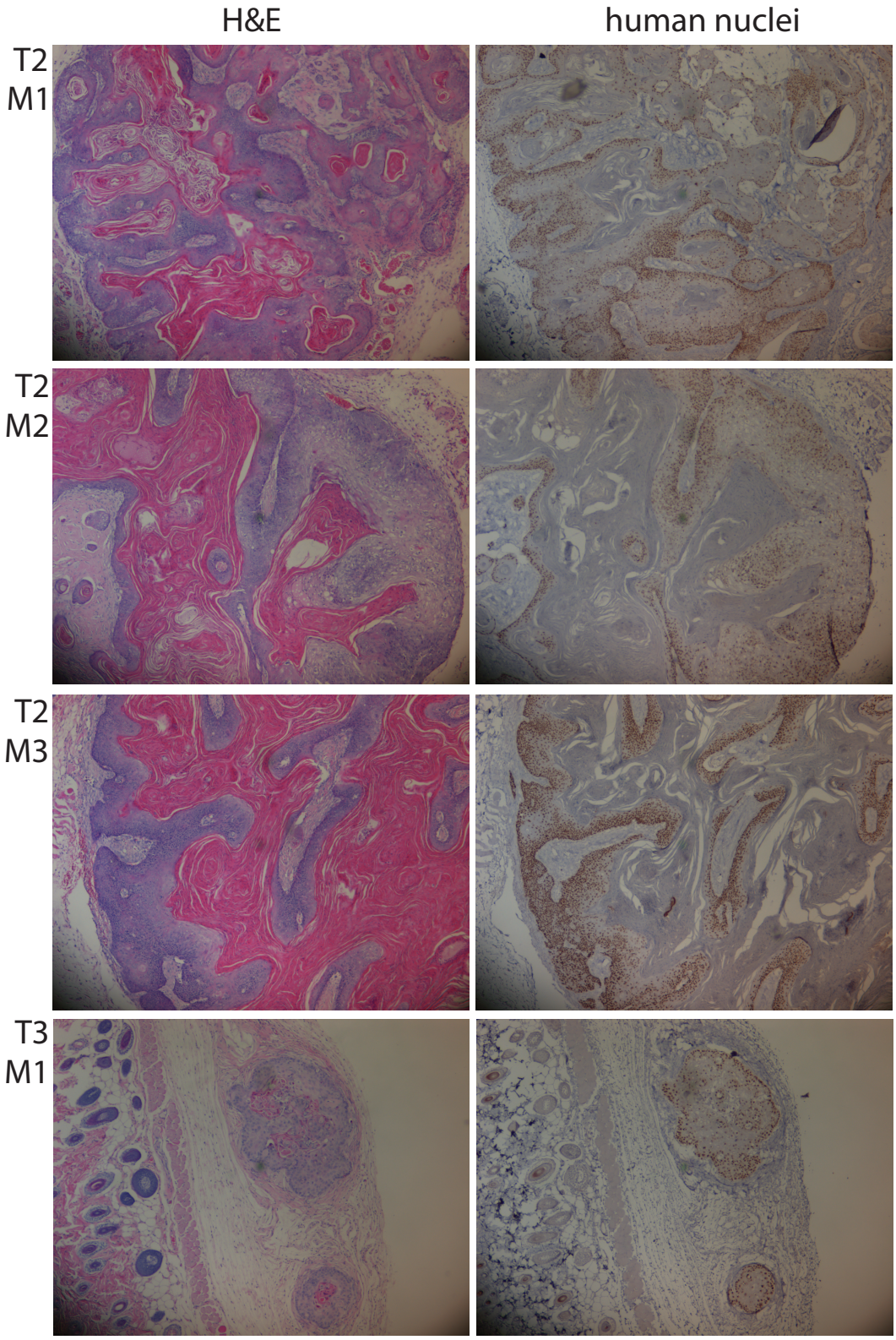

Figure S10. HNSCC-derived organoids result in tumor formation in vivo.

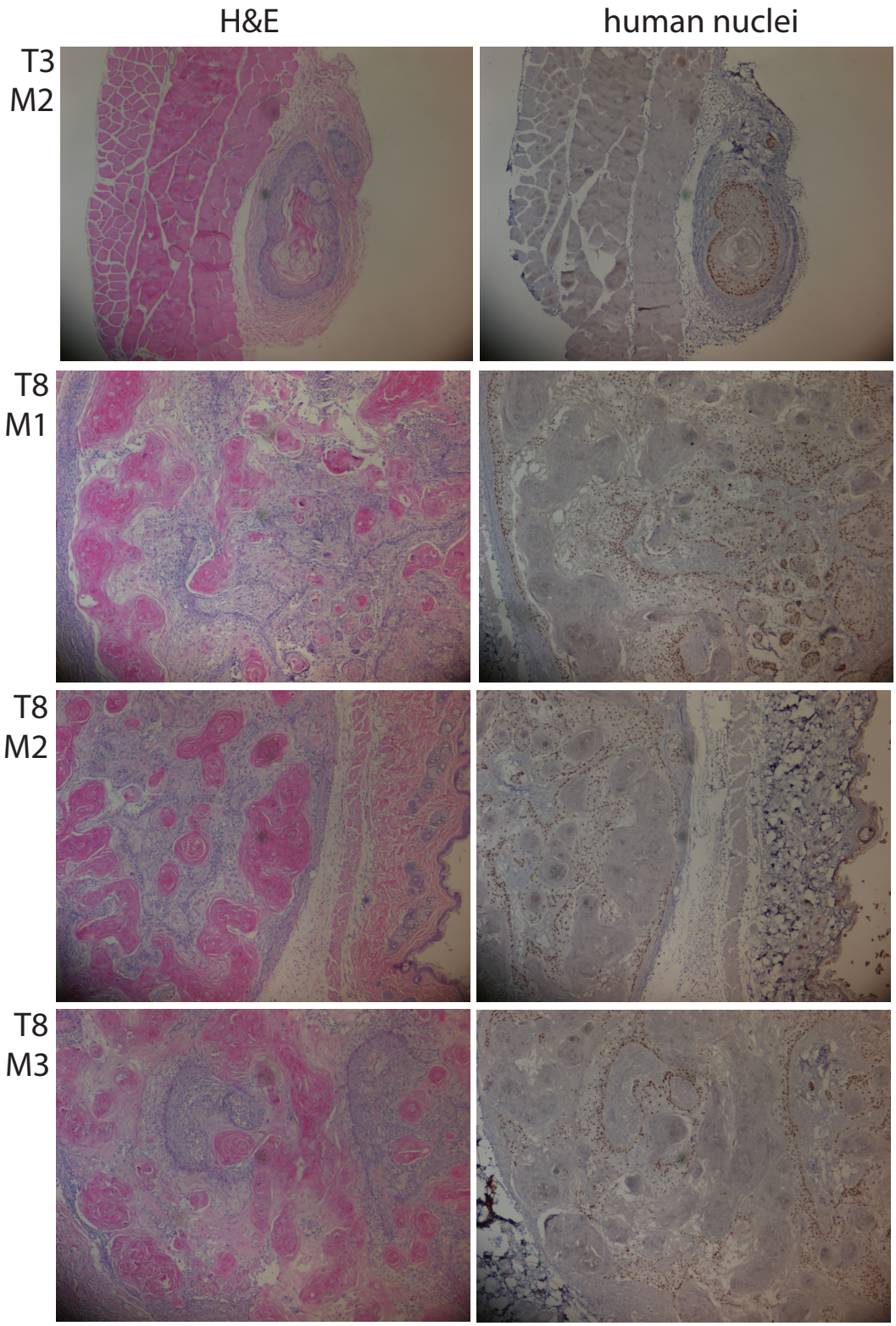

Figure S10. HNSCC-derived organoids result in tumor formation in vivo, related to Figure 5. For all transplanted organoid line, three mice were injected. Here, H&E and anti-human nuclei staining for these tumors is shown. As can be seen, histology of tumors originating from the same organoid line matches. Scale bar, 100 µm.

Figure S11. In vitro drugscreens in HNSCC-derived organoids.

a

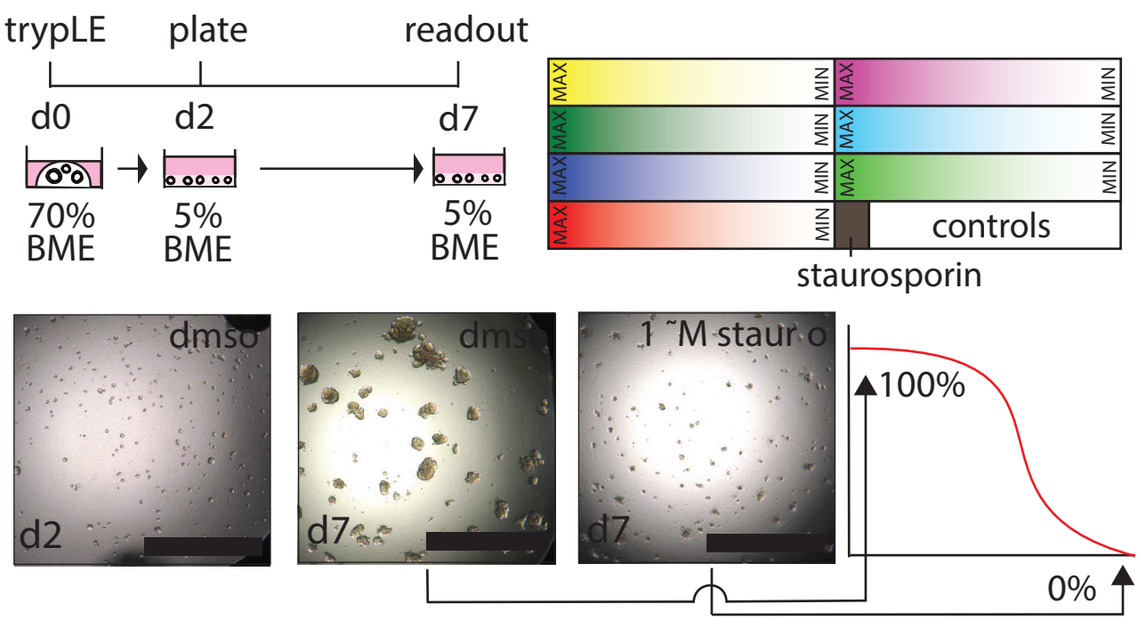

b

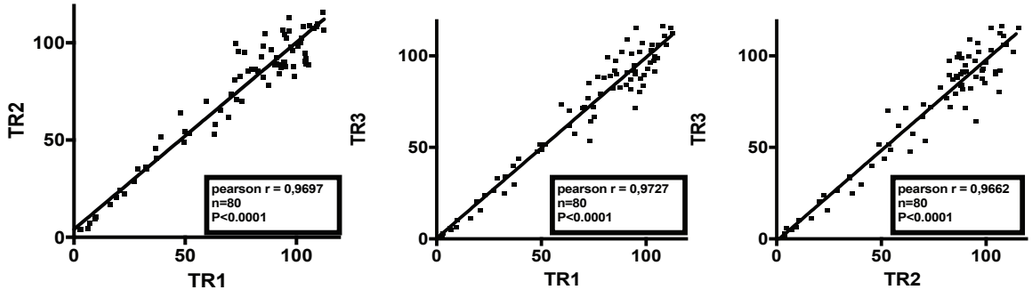

c

Drug used:	T1	T2	T3	T4	T5	T6	T7	T8	T9	T24	T25	T27	T28
Cisplatin	0.72	0.72	0.34	0.77	0.71	0.65	0.71	0.92	0.79	0.82	0.64	0.60	0.57
Carboplatin	0.72	0.67	0.34	0.77	0.71	0.65	0.71	0.92	0.79	0.82	0.64	0.60	0.57
Cetuximab	0.82	0.82	0.63	0.74	0.90	0.72	0.76	0.47	0.59				
Alpelisib	0.67	0.41	0.32	0.71	0.60	0.62	0.81	0.88	0.46	0.96	0.81	0.50	0.70
AZD4547	0.76	0.41	0.85	0.71	0.60	0.78	0.81	0.88	0.46	0.96	0.81	0.50	0.70
Everolimus	0.76	0.41	0.30	0.71	0.70	0.78	0.81	0.88	0.77	0.96	0.81	0.50	0.70
Nutlin	0.76	0.41	0.85	0.71	0.60	0.78	0.81	0.88	0.77	0.96	0.81	0.50	0.70
Niraparib	0.76	0.62	0.85	0.71	0.60	0.78	0.81	0.88	0.46	0.96	0.81	0.50	0.70
Vemurafenib				0.74	0.43			0.59	0.86				

Figure S11. In vitro drug screens in HNSCC-derived organoids, related to Figure 6. A. Schematic layout of the drug screens as performed in this study. Organoids were disrupted into single cells on day 0, and plated to recover for two days. On day 2, organoids were collected from the BME, washed, filtered, counted and plated in 5% BME in organoid medium in 384 well format (500 organoids per well). Subsequently a gradient of drug concentrations was printed in the wells (different drugs are represented by different colors in the figure), and cells were left exposed to the drugs for five days. As positive control, cells were exposed to 1 µM staurosporin. Solvent volumes were normalized for each plate, so that percentage DMSO or PBS/Tween-20 was identical for each well. Wells with only normalization were used as negative control. Each drug concentration was tested in triplicate. Readout was performed using Cell Titer Glow. B. To assess the reproducibility of the assay, the same drug screen was performed three times (technical replicates, named as TR1, TR2 and TR3). Calculated viability for each individual data point was plotted against its replicate value to assess robustness of the assay. C. Z factor scores of the performed drug screens for all drugs and all organoid lines presented in this work.

Figure S12. Sensitivity of HNSCC-derived organoids exposed to compounds used in this study.

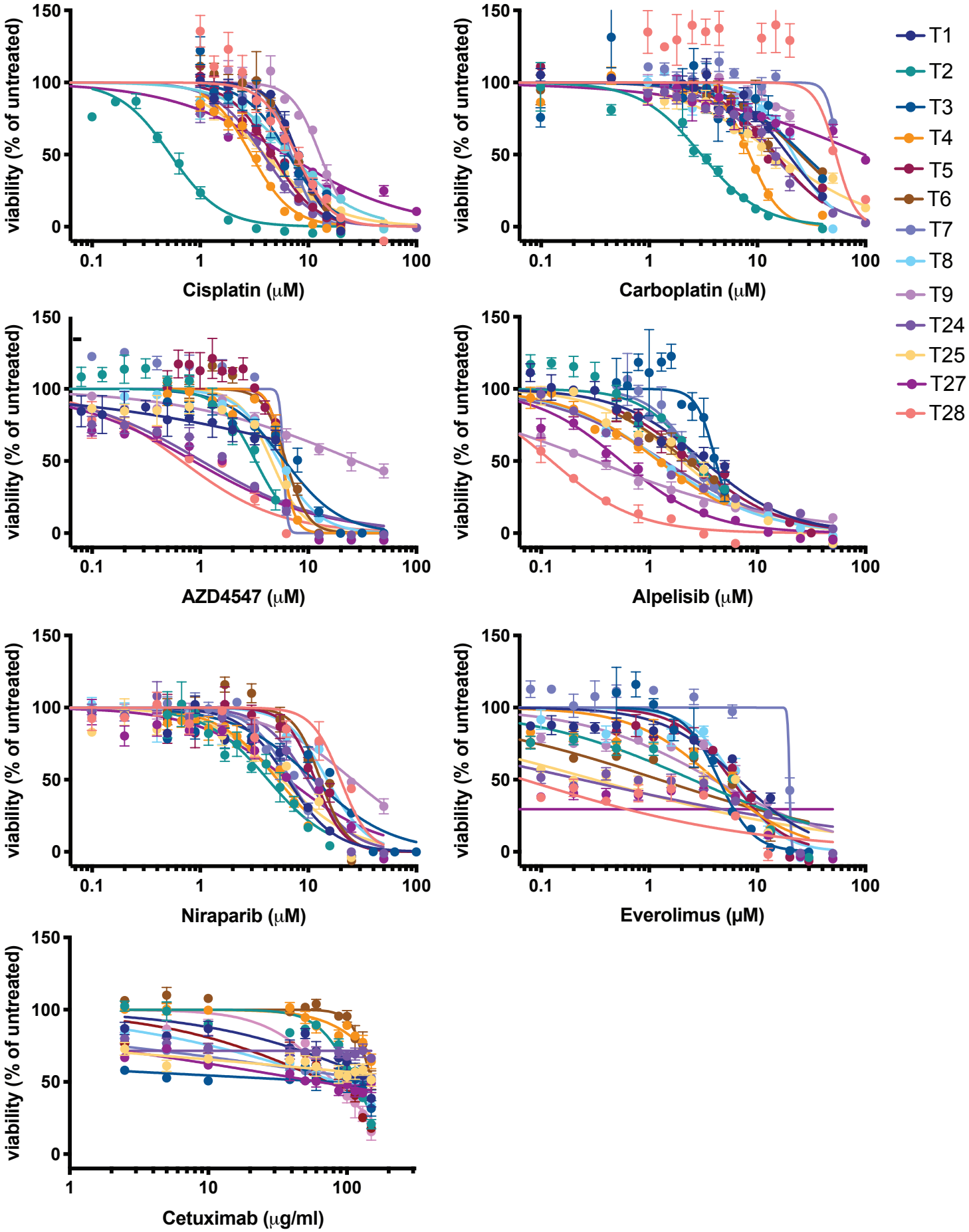

Figure S12. Sensitivity of HNSCC-derived organoids exposed to all compounds used in this study, related to Figure 6. Drugscreen results from organoid lines exposed to Cisplatin, Carboplatin, Cetuximab, AZD4547, Everolimus, Alpelisib and Niraparib.

Figure S13. Differential gene expression between organoids showing a good or poor response to cisplatin/carboplatin, cetuximab or radiotherapy.

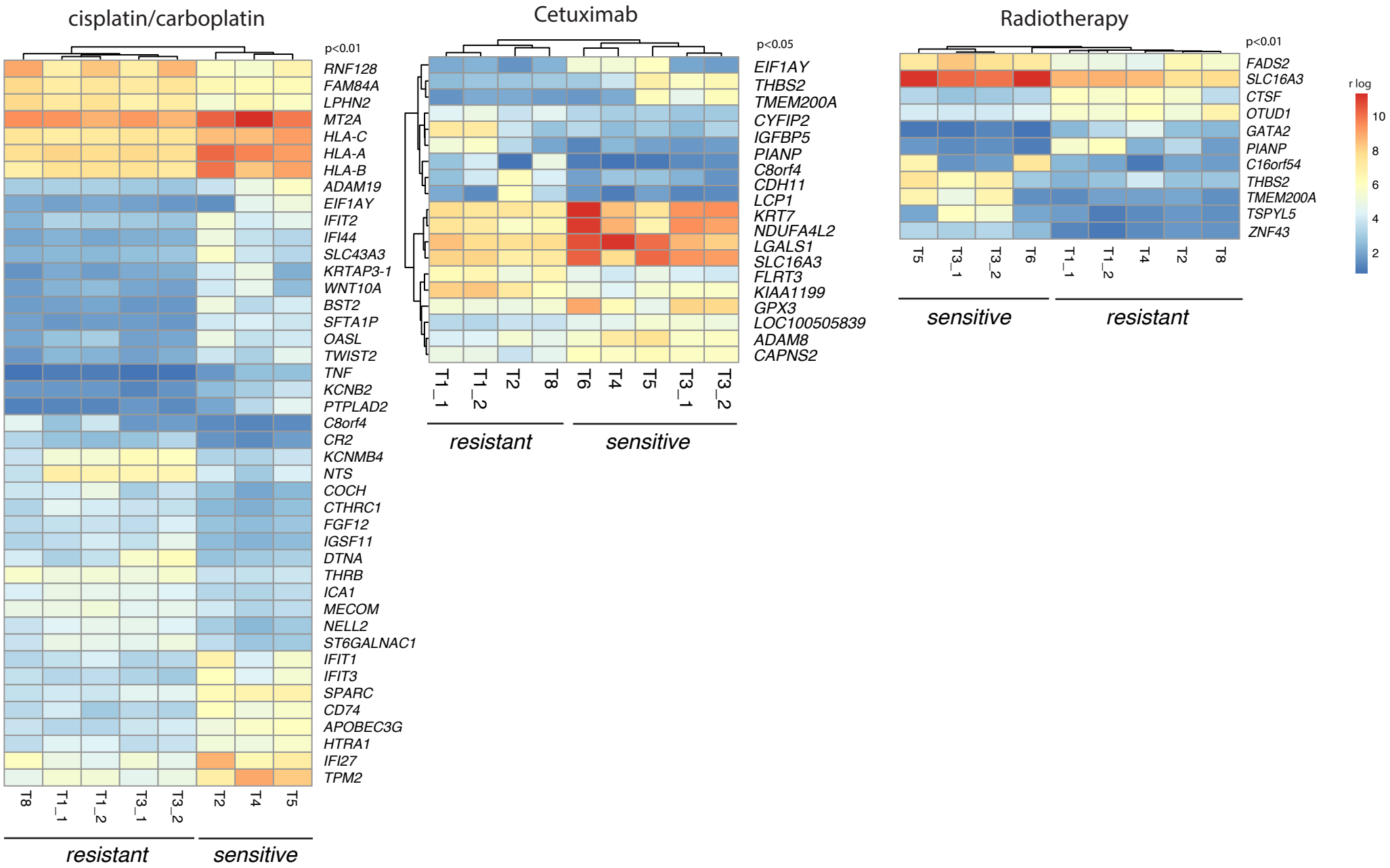

Figure S13. Diferential gene expression between organoids showing a good or poor respons to cisplatin/carboplatin, cetuximab or radiotherapy, related to figure 6. . Heatmap showing differentially expressed genes between good and bad responding organoid lines. Only genes with a padj < 0.001 are shown here. DEseq analysis results in identification of genes differentially expressed between lines that are most and least sensitive, respectively. to the therapy of interest. Here, cisplatin/carboplatin, cetuximab and radiotherapy are tested.

Figure S14. Chemoradiation therapy in ten HNSCC organoid lines, related to Figure 6.

A

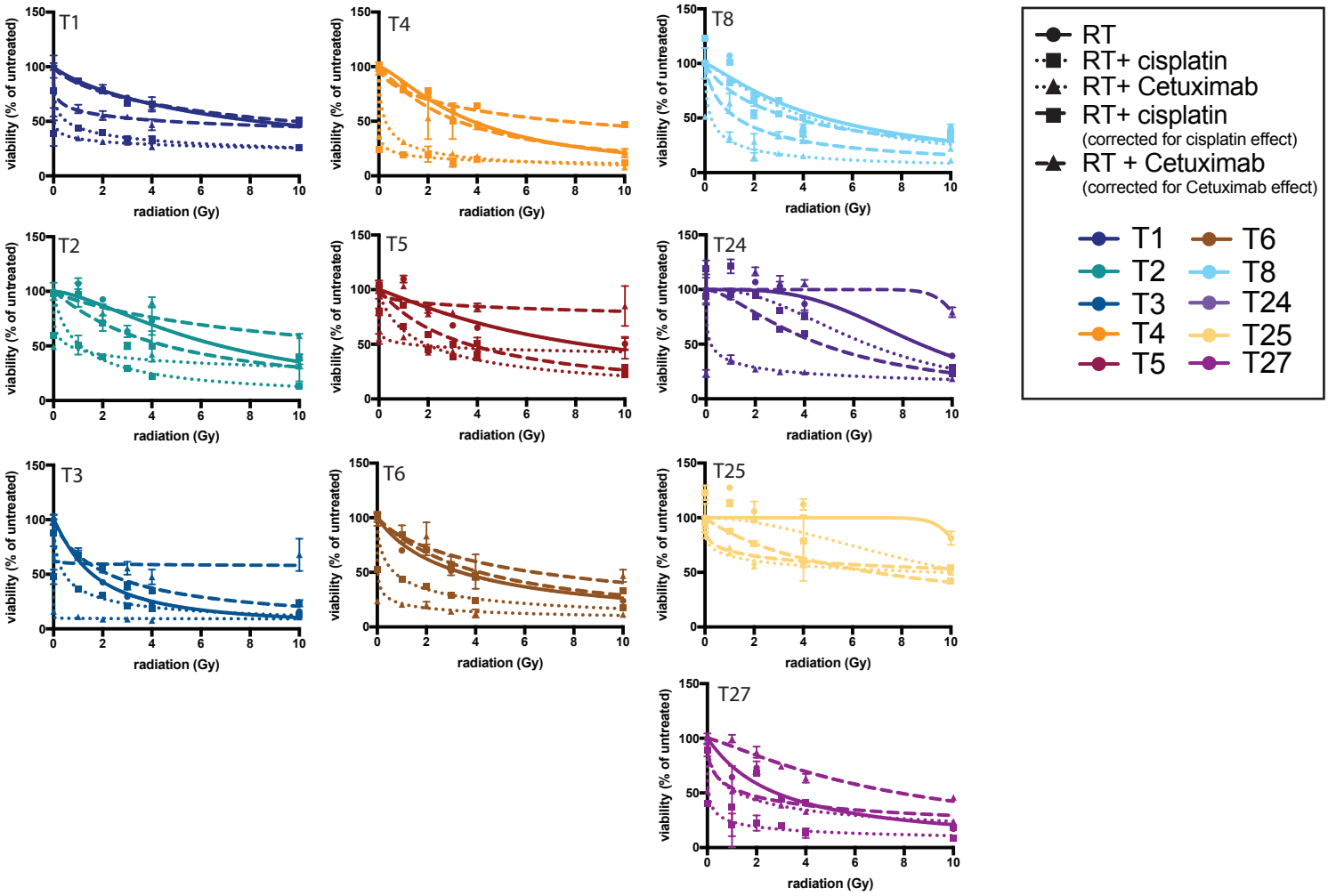

B

	T3	T24	T6	T4	T8	T1	T2	T5	T27	T25
RT only AUC	316.4	428	477.7	489.2	557.9	651.3	682.7	688.4	835.6	1029
RT in the presence or cisplatin AUC	401.4	394.3	523.4	622.8	506.1	654.6	557.9	511.7	560.1	617.6

low high

C

	T3	T24	T6	T4	T8	T1	T2	T5	T27	T25
RT only AUC	316.4	428	477.7	489.2	557.9	651.3	682.7	688.4	835.6	1029
RT in the presence or Cetuximab AUC	600.4	670.9	594	471.7	347.2	526	787.9	858.2	1035	619.9

low high

D

	T24	T3	T8	T5	T6	T2	T27	T25	T4	T1
RT + Cis AUC	394.3	401.4	506.1	511.7	523.4	557.9	560.1	617.6	622.8	654.6
RT AUC	428	316.4	557.9	688.4	477.7	682.7	835.6	1029	489.2	651.3
Cisplatin IC50	3.8	6.6	6.9	6.9	7.8	0.5	6.2	4.0	3.0	7.9

low high

E

	T8	T4	T1	T6	T3	T25	T24	T2	T5	T27
RT+ Cet AUC	347.2	471.7	526	594	600.4	619.9	670.9	787.9	858.2	1035
RT AUC	557.9	489.2	651.3	477.7	316.4	1029	428	682.7	688.4	835.6
Cetuximab AUC	119.4	170.5	137.5	180.7	93.64	112.6	129.5	152	121.4	104.1

low high

Figure S14. Chemoradiation therapy in ten HNSCC organoid lines, related to Figure 6. A. Kill curves of all ten tested lines, exposed to radiotherapy (RT) alone, or in combination with cisplatin or Cetuximab. B, Heatmap depicting AUC of RT alone or combined with cisplatin, corrected for the effect of chemotherapy alone. C. Heatmap depicting AUC of RT alone, or combined with Cetuximab, corrected for the effect of chemotherapy alone. D. Heatmap depicting AUC of RT alone, cisplatin alone, or RT + Cisplatin, not corrected for the effect of chemotherapy alone. E. Heatmap depicting AUC of RT alone, Cetuximab alone, or RT + Cetuximab, not corrected for the effect of chemotherapy alone. Blue indicates low AUC values, red indicates high AUC values.

Figure S15. Sensitivity of matched normal and tumor organoids to compounds used in this study.

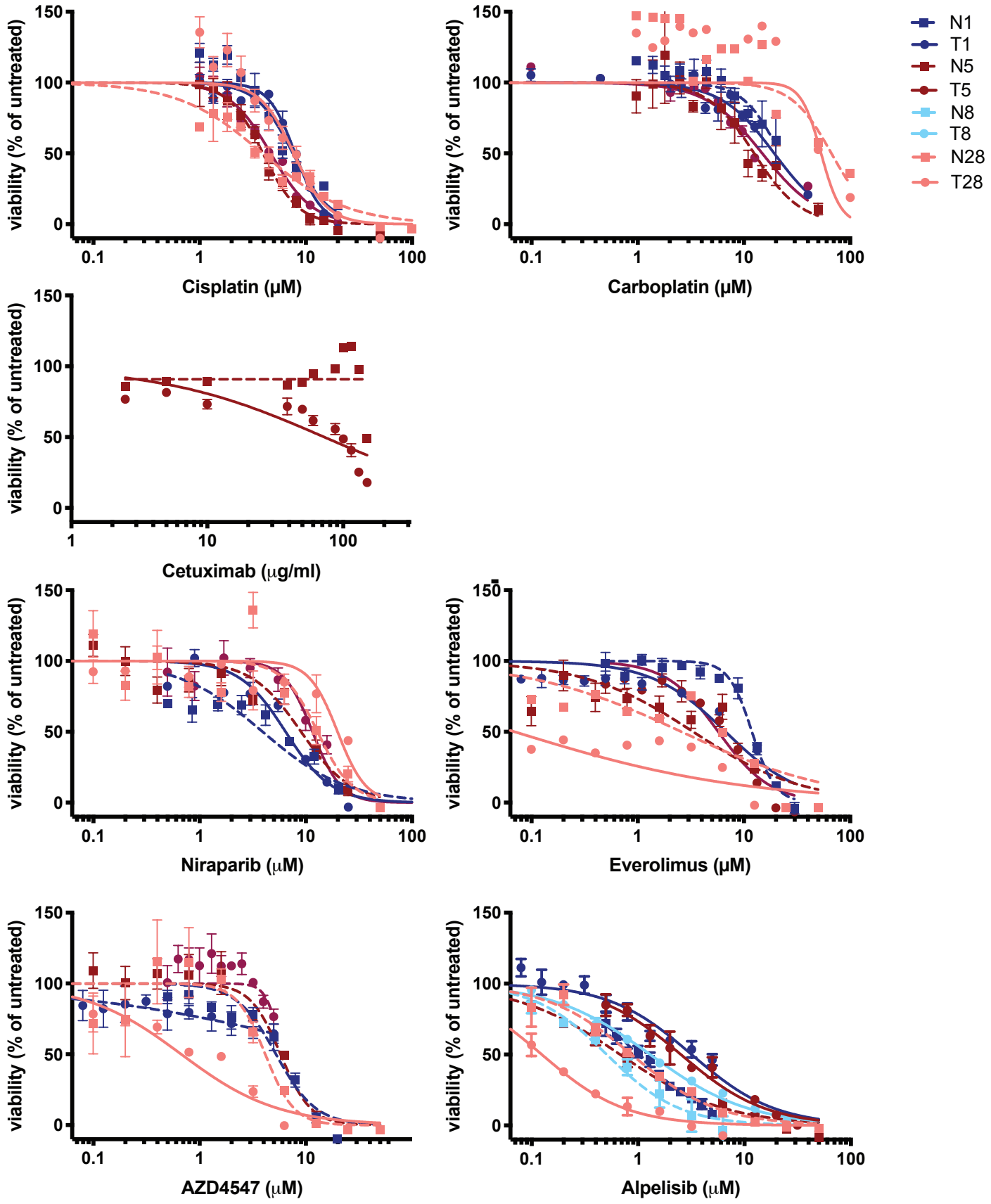

Figure S15. Sensitivity of matched normal and tumor organoids to compounds used in this study, related to Figure 7.
Drugscreen results from N1 and T1, N5 and T5, N8 and T8 and N28 and T28 organoid lines exposed to cisplatin, carboplatin, cetuximab, Niraparib, Everolimus, AZD4547 and Alpelisib.

Figure S16. Organoid in vitro drug response, remains comparable over time in culture.

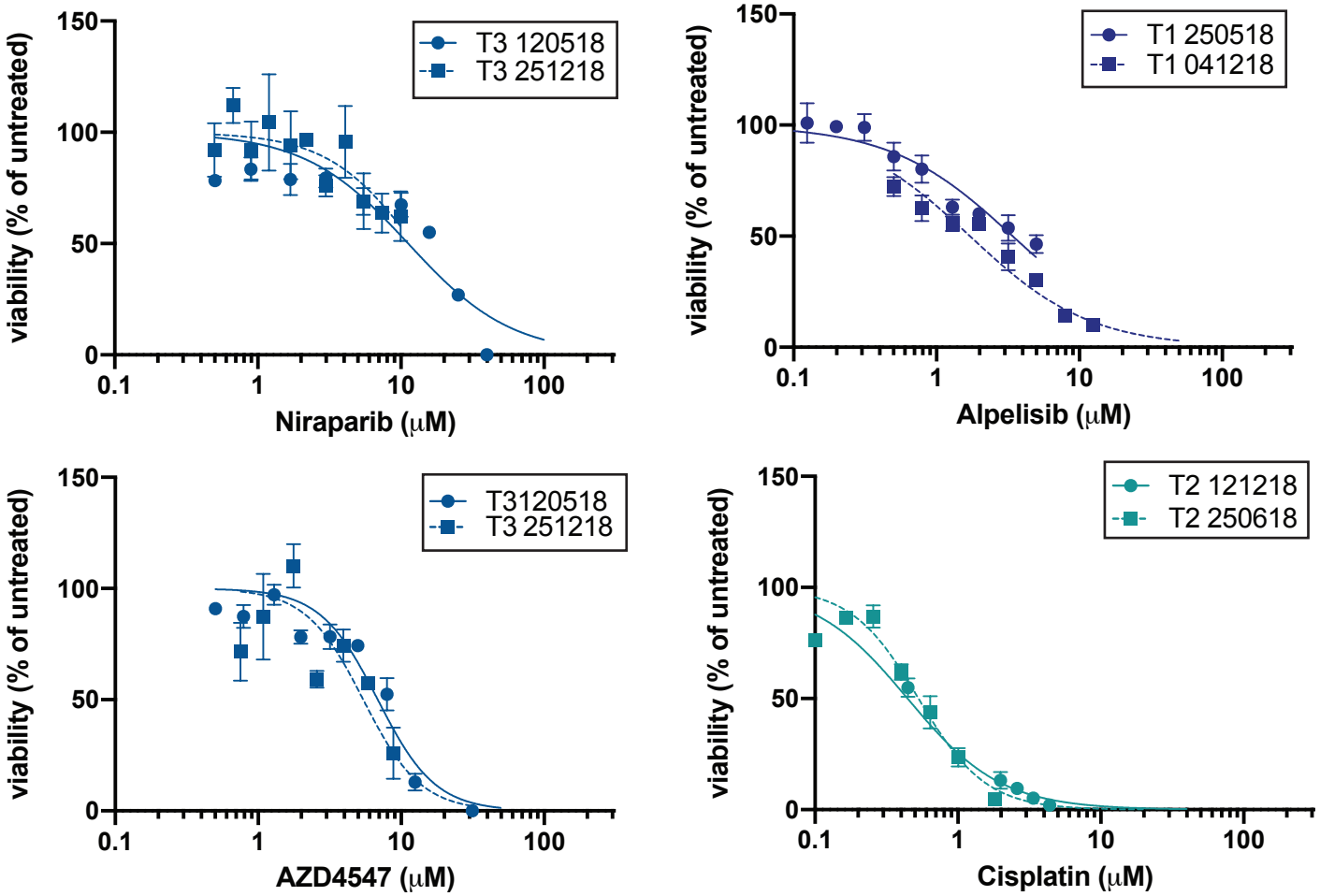

Figure S16. Organoid in vitro drug response remains comparable over time in culture, related to Figure 6 and 7. Four different drugscreens were performed with at least 22 weeks of culturing in between, and reveal comparable drug screening results over time. Screens shown are Alpelisib testing in T1, Cisplatin testing in T2 and Niraparib and AZD4547 testing in T3.

Table S1. Patient clincal data, related to Figure 2A

#T	gender	birthyear	tumor location	pretreatment	HPV status	sequencing	drugscreen	N/T	No longer in culture
1	male	1955	tongue	no	negative	oncopanel	Yes	N/T	
2	female	1927	larynx	no	negative	oncopanel	Yes	T	
3	female	1934	larynx	no	negative	oncopanel	Yes	T	
4	male	1956	tongue	no	negative	oncopanel	Yes	T	
5	male	1938	parotis SCC	no	negative	exome sequencing	Yes	N/T	
6	male	1935	oral cavity	no	negative	oncopanel	Yes	T	
7	female	1960	floor of mouth	no	negative	oncopanel	Yes	T	
8	female	1948	gingiva	no	negative	exome sequencing	Yes	N/T	
9	male	1948	mandibula	no	negative	oncopanel	Yes	T	
10	female	1936	mandibula	no	n.t.	oncopanel	No	T	stopped at p10
11	male	1951	oral cavity	no	n.t.	n.t.	No	T	stopped at p20
12	male	1937	gingiva	no	n.t.	n.t.	No	T	
13	male	1946	larynx	no	n.t.	n.t.	No	T	
14	female	1962	larynx	no	n.t.	n.t.	No	T	stopped at p4
15	male	1954	pharynx	no	n.t.	n.t.	No	T	
16	male	1959	pharynx	no	n.t.	n.t.	No	T	
17	male	1939	floor of mouth	no	n.t.	n.t.	No	N	
18	male	1949	larynx	no	n.t.	n.t.	No	N	
19	male	1949	oropharynx	no	n.t	n.t.	No	T	
20	male	1954	salivary gland SCC	no	n.t.	oncopanel	No	N/T	
21	female	1947	larynx	no	n.t.	n.t.	No	T	stopped at p5
22	male	73	pharynx	no	negative	n.t.	No	T	
23	male	1970	floor of mouth	no	n.t.	n.t.	No	T	
24	male	1941	oral cavity	no	n.t.	oncopanel	Yes	T	
25	male	1946	floor of mouth	no	n.t.	oncopanel	Yes	T	
26	male	1947	nasal cavity	no	n.t.	oncopanel*	no	T	
27	female	1958	oral cavity	no	n.t.	oncopanel	Yes	N/T	

28	male	1935	oral cavity	no	n.t.	oncopanel	Yes	N/T	
29	male	1943	neck	no	n.t.	oncopanel	Yes	N/T	
30	male	1947	hypopharynx	no	n.t.	n.t.	No	T	
31	female	1932	tongue	no	n.t.	n.t.	No	N	
32	female	1939	larynx	no	n.t.	n.t.	No	T	
34	female	1972	larynx	no	n.t.	n.t.	No	T	stopped at p5
35	male	1965	oral cavity	no	n.t.	n.t.	No	N	stopped at p6

- No mutations were detected by the 54 gene covering oncopanel. WGS will be performed to validate the tumor origin of this organoid line.

Table S1. Patient clinical data, related to Figure 2A. Patient data corresponding to the organoid lines presented in this work.

Table S3: Detected mutations in genes checked in the OncoAMP panel, related to Figure 4.

organoid line	gene	DNA	protein	variant effect	external status
T1	PIK3CA	1633G>A	Glu545Lys	missense	COSM763
T1	TP53	586C>T	Arg196*	stop gained	COSM10705
T2	KRAS	204G>T	Arg68Ser	Missense	COSM183929
T2	ESR1	1138G>A	Glu380Lys	Missense	
T2	TP53	406C>T	Gln136*	Stop gained	COSM11166
T2	TP53	374C>T	Thr125Met	Missense	COSM44988
T3	TP53	102delC	Leu35Cysfs*9	Frameshift	COSM2745164
T3	FGFR2	1576A>G	Lys526Glu	Missense	rs121918507
T4	HRAS	37G>C	Gly13Arg	Missense	COSM486
T4	TP53	578A>G	His193Arg	Missense	COSM10742
T6	CDKN2A	151G>A		splice acceptor	COSM13694
T6	TP53	637C>T	Arg213*	stop gained	COSM10654
T6	TP53	856G>A	Glu286Lys	Missense	COSM10726
T7	KRAS	35G>C	Gly12Arg	Missense	COSM522
T7	PIK3CA	1633G>A	Glu545Lys	Missense	COSM763
T7	MET	504G>T	Glu168Asp	Missense	COSM706
T7	TP53	830G>A	Cys277Tyr	Missense	COSM43737
T9	BRAF	1799T>A	Val600Glu	Missense	COSM476
T9	PIK3CA	3140A>G	His1047Arg	Missense	COSM775
T10	BRAF	1799T>A	Val600Glu	Missense	COSM476
T10	PIK3CA	3140A>G	His1047Arg	Missense	COSM775
T20	VHL	74C>T	Pro25Leu	Missense	COSM36211
T24	KRAS	34G>C	Gly12Arg	Missense	COSM518
T24	TP53	586C>T	Arg196*	Missense	COSM10705
T24	PIK3CA	1624G>A	Glu542Lys	Missense	COSM760

T24	PDGFRA	827C>T	Thr276Met	Missense	COSM1540243
T25	KRAS	34G>C	Gly12Arg	Missense	COSM518
T25	PIK3CA	3140A>G	His1047Arg	Missense	COSM775
T25	TP53	694A>T	Ile232Phe	Missense	COSM562650
T27	ATM	5558A>T	Asp1853Val	Missense	COSM3752120
T27	ATR	2875G>A 2290A>G 946G>A	Val959Met, Lys764Glu, Val316Ile	Missense	COSM1579027 COSM5020937 COSM1579030
T27	EGFR	G761A	Arg254Lys	Missense	COSM5830713
T27	ERBB2	1960A>G	Ile654Val	Missense	COSM6854579
T27	KDR	889G>A	Val297Ile	Missense	COSM1131107
T27	MPL	340G>A	Val144Met	Missense	COSM3996746
T27	PDGFRA	1432T>C	Ser478Pro	Missense	
T27	RET	166C>A	Lys56Met	Missense	COSM6493950
T28	MDM2	428G>A	Asp140Asn	Missense	
T28	TP53	836_848delGGAGAGACCGGCG	Gly279AlafsTer62	Frameshift	
T29	PIK3CA	1633G>C	Glu545Gln	COSM27133	COSM27133
T29	TP53	375G>T		Splice region	COSM381996
T29	TP53	825T>A	Val272Glu	Missense	COSM44580

Table S3. Detected mutations in genes checked in the OncoAMP panel, related to Figure 3. Details of mutation detected by (targeted) sequencing of the organoid lines.

Table S6. Patient information for correlation between in vitro organoid response to RT and patient clinical response.

organoid/ patient	tumor location	tumor stage	primary surgery	primary / adjuvant RT	indication for adjuvant RT	RT dose	last check of response (after end RT)	timing of first indication of relapse after RT	details	organoid sensitive for RT	match organoid response/ patient response
T1	tongue	T2N2b	excision of primary tumor, selective neck dissection level I-IV right and reconstruction with free radial forearm flap	adjuvant	positive resection margins, multiple lymph node metastases with extranodal extension	66 Gy	12 months	6 months	succumbed to locoregional and distant disease 12 months after RT completion	no	yes
T2	larynx	T2N0		primary		60 Gy	18 months	4 months	total laryngectomy for recurrence, thereafter no evidence of disease	no	yes
T3	larynx	T3N0		primary		48 Gy*	5 months	n.a.	succumbed to lung adenocarcinoma 5 months after end of RT without signs of laryngeal recurrence	yes	yes
T5	parotid gland	T4aN0	parotidectomy	adjuvant	positive margins	66 Gy	11 months	n.a.	no evidence of disease	yes	yes
T8	gingiva	T4aN0	excision of primary tumor with marginal mandibula resection and selective neck dissection level I-III left	adjuvant	positive margins	66 Gy	6 months	n.a.	no evidence of disease	no	no
T25	floor of mouth	T2N1	excision of primary tumor, selective neck dissection level I-III both sides and reconstruction with free radial forearm flap	adjuvant after complete neck dissection because of neck recurrence	recurrence neck	52 Gy	2 months	1 month	succumbed to metastases neck, skin, lungs and liver	no	yes
T27	floor of mouth	T3N1	excision of primary tumor and sentinel node biopsy	adjuvant	close surgical margins and positive sentinel node	56	2 months	n.a.	no evidence of disease	yes	yes

* limited RT dose because of diagnosis of second primary lung adenocarcinoma

Table S6. Patient information for correlation between in vitro organoid response to RT and patient response, related to Figure 6.

Table S7. Antibodies used for immunohistochemistry

protein	Supplier	Ordernumber	Host Species	Clone	Lotnumber	Dilution	Pretreatment
KRT5	Novocastra	NCL-L-CK5	Mouse	XM26	6027941	Ventana 1:200	CC1 24' (EDTA) Ventana
MKI67	Monosan	MONX10293	Mouse	MM1	10293	1:2000	Citrate autoclave
TP40	Abcam	ab172731	Rabbit	BC28	GR322490-1	Ventana 1:50	CC1 48'/ 32'AB
P53	DAKO	M7001	Mouse	DO-7	95381	Ventana 1:6000	CC1 24' (EDTA) Ventana
P63	Abcam	AB735	Mouse	4AB	AB735	1:800	Citrate
Human nuclei	Abcam	AB190710	Mouse	NM95	GR3199786-1	1:500	Citrate autoclave
KRT13	Progen	10523	Mouse	1C7	10523	1:100	Citrate
dTOM	Rockland	600-401-379	Rabbit			1:1000	Citrate

Table S7. Antibodies used for immunohistochemistry, related to method section.

Legend of supplementary Movies and Table S2, S4 and S6

Supplemental Movie S1. Time lapse showing organoid outgrowth after plating cells obtained from tissue digestion, related to Figure 1. Movie is a three day timelapse of cultures isolated 24h before the start of the movie for primary tissue.

Supplemental Movie S2. Outgrowth of organoids from single cells or clumps of cells after splitting an established organoid line, related to Figure 1. Movie is a three day timelapse of organoids that were splitted 2 hours prior to the start of imaging with TrypLE.

Supplemental Movie S3. Infection of organoids with dTOM-HSV, related to Figure 1. Movie is a 62 hours timelapse of organoids infected one hour before the start of imaging with dTOM-HSV. Scalebar 500 µm.

Supplemental Movie S4. Example of a timelapse movie of H2B-mNEON N1 organoids, used to quantify segregation errors during mitosis, related to Figure 4. Color in the left panel indicates depth. Scalebar 20 µm.

Supplemental Movie S5. Example of a timelapse movie of H2B-mNEON N1 organoids, used to quantify segregation errors during mitosis, related to Figure 4. Color in the left panel indicates depth. Scalebar 20 µm.

Table S2. DEseq2 analysis results comparing tumoroid samples versus normal wildtype organoids, related to Figure 2.

Table S4. Mutations detected in T5 and T8 organoids and corresponding tumor tissue by whole exome sequencing, related to Figure 3.

Table S5. DEseq2 analysis identifying differential gene expression analysis performed on organoids responding well or poorly to cisplatin/carboplatin, cetuximab or radiotherapy, related to Figure 6.